

Electronic Supplementary Information (ESI)

for

Fabrication of transferrin modified two-photon gold nanoclusters with near-infrared fluorescence and its application for bioimaging

Kangdi He,^a Shengrong Yu,^{*,a, b} Xiao Wang,^c Dian Li,^a Jia Chen,^a Hongmei Zhong,^a
Qing Xu,^a Yong-Xiang Wu,^{*,a, b} and Ning Gan^{*,a}

^a. State Key Laboratory Base of Novel Functional Materials and Preparation Science,
Key Laboratory of Advanced Mass Spectrometry and Molecular Analysis of Zhejiang
Province, School of Materials Science and Chemical Engineering, Ningbo University,
Ningbo, Zhejiang, 315211, China.

^b. Institute of Mass Spectrometry, Ningbo University, Ningbo, Zhejiang 315211, China

^c. Immunology Innovation Team, School of Medicine, Ningbo University, Ningbo,
Zhejiang 315211, China

* To whom correspondence should be addressed.

E-mail: yushengrong@nbu.edu.cn

wuyongxiang@nbu.edu.cn

ganning@nbu.edu.cn

Table of contents

1. Materials and reagents.....	S-3
2. Apparatus.....	S-3
3. Synthesis of Tf-AuNCs.....	S-4
4. Synthesis of MnO ₂ nanosheets.....	S-4
5. Preparation of the nanoprobe Tf-AuNCs@MnO ₂ and detection of GSH in buffer solution.....	S-4
6. Cell culture and cytotoxicity assessment test.....	S-5
7. Single-photon bioimaging of the nanoprobe Tf-AuNCs@MnO ₂ toward endogenous GSH in living cells and tissue.....	S-5
8. Two-photon bioimaging of the nanoprobe Tf-AuNCs@MnO ₂ toward endogenous GSH in living cells and tissue.....	S-6
9. Synthesis of Two-photon silica nanoparticles (TP-SiNPs) and two-photon fluorescence imaging of TP-SiNPs in mouse liver tissue.....	S-6
10. MRI response of the nanoprobe Tf-AuNCs@MnO ₂ toward GSH in buffer solution and endogenous GSH in cells.....	S-7
11. Supplementary figures and table.....	S-8
12. References.....	S-27

1. Materials and reagents

Hydrogen tetrachlorocuprate (III) trihydrate ($\text{HAuCl}_4 \cdot 3\text{H}_2\text{O}$) was purchased adamas-beta (Shanghai, China). Apo-transferrin, Ethyldiisopropylamine (DIPEA), 2-(7-Azabenzotriazol-1-yl)-*N,N,N',N'*-tetramethyluronium hexafluorophosphate (HATU), (3-aminopropyl)triethoxysilane (APTES), Tetraethyl orthosilicate (TEOS), Triethanolamine, Glutaric Anhydride and 2-Naphthoic acid were obtained from Sigma-Aldrich (St. Louis, MO). Manganese chloride (MnCl_2), lipoic acid (ALA), glutathione (GSH), *N*-ethylmaleimide (NEM) purchased from Aladdin (Shanghai, China). Potassium chloride (KCl), Sodium hydroxide (NaOH), sodium chloride (NaCl), zinc sulfate (ZnSO_4), magnesium sulfate (MgSO_4), potassium nitrate (KNO_3) was obtained from macklin (shanghai, China). Homocysteine (Hcy), Glycine (Gly), Cysteine (Cys) and Glutamic acid (Glu) purchased from Solarbio. Hydrogen peroxide (H_2O_2) and Tetramethylammonium hydroxide (TMAOH) were purchased from Sinopharm reagent. All deionized water is obtained through Milli-Q system. Dulbecco's modified Eagle's high glucose (DMEM) medium purchased from Thermo Fisher scientific.

2. Apparatus

The transmission electron microscopy (TEM) images of Tf-AuNCs, MnO_2 nanosheets and Tf-AuNCs@ MnO_2 nanoprobe were obtained on a JEM-2100F transmission electron microscope (Jeol, Tokyo, Japan) with an accelerating voltage of 200 kV. The energy-dispersive X-ray spectroscopy (EDS) is measured by Thermo Scientific NORANTM System 7. Dynamic light scattering (DLS) analysis was conducted on a Malvern Zeta sizer Nano ZS90 (London, U.K). A Bruker AXS D8 ADVANCE XRD (Karlsruhe, Germany) was employed to record the powder X-ray diffraction (XRD) spectra. X-ray electron spectroscopy (XPS) is measured in Thermo Scientific equipped with Al $\text{K}\alpha$ X-ray source ($h\nu=1486.6$ eV). The UV-vis spectra were recorded on a UV-1800 spectrophotometer (Shimadzu, Kyoto, Japan). Fourier Transform infrared spectrum (FT-IR) analysis was performed on Nicolet 6700 infrared spectrometer, purchased from Madison Co., Ltd. Fluorescence spectra were collected on an RF-6000 fluorescence spectrophotometer (Shimadzu, Kyoto, Japan). The

fluorescence lifetimes of Tf-AuNCs were determined on an FLS980 spectrometer (Edinburgh, U.K.). The Cell Counting Kit-8 (CCK-8) assay was performed using Varioskan Flash microplate reader (Thermo Fisher Scientific) at 450 nm. The single-photon confocal microscope image was obtained from a Leica SP8 (Beijing, China). Two-photon confocal fluorescence images were obtained by using Olympus FV1200MPE multiphoton laser scanning confocal microscope. The MRI response signals were measured at 0.5 T on an MesoMR23-060H-I equipment.

3. Synthesis of Tf-AuNCs

All glass vessels were used after washing with aqua regia. Firstly, 200 μL HAuCl_4 (25 mM) was added 1.0 mL of PBS solution containing 25 mg/mL transferrin. The mixed solution was shaken for 2-3 min, and then 800 μL NaOH solution (0.1 M) was added and shaken for 2-3 min. subsequently, the mixture incubated at 37 $^\circ\text{C}$ for 12 h. Under UV light irradiation, the solution emits red fluorescence indicating the formation of Tf-AuNCs. Tf-AuNCs solution was centrifuged in an ultrafiltration centrifuge tube with a molecular weight of 10000 for 30 min, and washed with deionized water three times. Tf-AuNCs solution was lyophilized for 48 h to obtain the dry products.

4. Synthesis of MnO_2 nanosheets

Firstly, 18 mL of TMAH solution (0.66 M) was mixed with 2.0 mL of H_2O_2 solution (30 wt %). Subsequently, the mixture was added to 10 mL of MnCl_2 (0.3 M) solution, and a dark brown precipitate was immediately formed. At room temperature, the mixture was stirred for 12 h in the dark. After the reaction was over, the product was precipitated by centrifugation at 10000 rpm, and washed with deionized water and ethanol three times. The dark brown precipitated bulk MnO_2 was freeze-dried for 24 h to remove the water. Taking 30 mg of dry bulk MnO_2 and adding 30 ml of distilled water to ultrasound for 15 h prepared 1.0 mg/mL of MnO_2 nanosheets stock solution.

5. Preparation of the nanoprobe Tf-AuNCs@ MnO_2 and detection of GSH in buffer solution

Tf-AuNCs (2.0 mg/mL) were mixed with different concentrations of MnO_2 nanosheets stock solution (1.0 mg/mL, 0-300 μL) to prepare nanoprobe with the different fluorescence quenching effects. Finally, 300 $\mu\text{g/mL}$ MnO_2 nanosheets chosen

as final concentration to form Tf-AuNCs@MnO₂ nanoprobe solution. The various concentrations of GSH in buffer solution was added to nanoprobe Tf-AuNCs@MnO₂. After 10 min of reaction, the fluorescence property of above reaction solution was measured by a RF-6000 fluorescence spectrophotometer with an excitation of 460 nm.

6. Cell culture and cytotoxicity assessment test

The living MCF-7 cells were obtained from Fudan University Shanghai Cancer Center (Shanghai, China). The MCF-7 cells was added the culture dish, a certain amount of DMEM medium was added culture vessel and the medium was changed every two days and culture in the cell incubator (37 °C, 5% CO₂, 95 % air).

MCF-7 cells were planted into 96 -well plates, 200 μL of cell suspension was added to each well(the cell concentration was $2.0 \times 10^5 \text{ mL}^{-1}$), cultured in a cell incubator for 24 hours, and different concentrations of nanoprobe Tf-AuNCs@MnO₂ were added to continue Cultivate for 24 h, remove the DMEM medium containing the nanoprobe, add CCK-8 (10 μL) containing DMEM medium and culture for 4 h, and finally measure the absorbance of each well with a microplate reader ($\lambda_{\text{abs}}=450 \text{ nm}$).

7. Single-photon bioimaging of the nanoprobe Tf-AuNCs@MnO₂ toward endogenous GSH in living cells and tissue

For single-photon confocal fluorescence imaging of endogenous GSH in living cells, the cells suspension (400 μL) was seeded in 24-well plates for 24 h. the cultured cells were washed with PBS solution three times and then incubated with the nanoprobe Tf-AuNCs@MnO₂ (300 μg/mL) for 6 h. After washing three times with PBS solution, the cells were fixed with 2% glutaraldehyde for 0.5 h. The cells subjected to fluorescence imaging measurements by single-photon confocal laser scanning microscope ($\lambda_{\text{ex}}=488 \text{ nm}$, $\lambda_{\text{em}}=620\text{-}780 \text{ nm}$). As a control group, the cell suspension was cultured with lipoic acid (500 μM) for 12 h, then incubated with the nanoprobe Tf-AuNCs@MnO₂ for 6 h, and then the intracellular GSH was imaged according to the above experimental method. As another control group, the cultured cells were pretreated 0.5 mM *N*-ethylmaleimide (NEM) for 4.0 h and then the intracellular GSH was imaged according to the above experimental method.

All mice were maintained in strict accordance according to the Animal Ethics Procedures and Guidelines of the People's Republic of China. All experiments were approved by the ethical committee of Ningbo University. The liver of mice was removed from the mouse. The liver tissues cut into slices with the thickness of 400 μm . The nanoprobe Tf-AuNCs@MnO₂ (3 mg/mL) was added to the slices and incubate for 4 h, then rinse three times with Dulbecco's phosphate buffered saline (DPBS) buffer. Next, the liver tissue incubated with nanoprobe was measured by a single-photon laser scanning confocal microscope ($\lambda_{\text{ex}}=488 \text{ nm}$, $\lambda_{\text{em}}=620\text{-}780 \text{ nm}$).

8. Two-photon bioimaging of the nanoprobe Tf-AuNCs@MnO₂ toward endogenous GSH in living cells and tissue

The previously cultured MCF-7 cells were incubated with the nanoprobe Tf-AuNCs@MnO₂ for 6 hours and fixed with glutaraldehyde (2.0 %). In the other two groups of controls, the cultured MCF-7 cells were treated with GSH inhibitors (NEM 0.5 mM) and promoters (ALA 0.5 mM), the treatment time was 4 h and 12 h, respectively. After that, the two groups of treated cells were incubated with nanoprobe for 6 hours, and then glutaraldehyde fixed the MCF-7 cells. In the three groups of experiments, the fluorescence changes in cell were measured by the Olympus multiphoton FV1200MPE confocal microscope. The excitation wavelength of the femtosecond laser was 920 nm. The emitted light signal was received under 620-780 nm.

The mouse liver was removed from mouse. The liver tissues cut into slices with the thickness of 400 μm . The treated liver slices were incubated with the nanoprobe Tf-AuNCs@MnO₂ for 6 h. Then, Liver tissue sections were washed with DPBS solution three times to remove nanoprobe that did not enter the cells. The Olympus multiphoton FV1200MPE confocal microscope was used to measure the two-photon fluorescence signal of liver tissue slices. The excitation wavelength of the femtosecond laser was 920 nm. The emitted light signal was received under 620-780 nm.

9. Synthesis of Two-photon silica nanoparticles (TP-SiNPs) and two-photon fluorescence imaging of TP-SiNPs in mouse liver tissue

The DMF solution (5.0 mL) containing 1.0 mL DIPEA and HATU (912.4mg, 1.2

mmol) was prepared. 2-Naphthoic acid (430.4 mg, 1.0 mmol) was added to the solution. After 30 min of reaction in an ice bath, the APTES (442 mg, 1.0 mmol) was added and stirred for 1 h at room temperature. The mixture was poured into ice water and the crude product was observed to be precipitated. The crude product was separated by vacuum filter and purified by silica gel column chromatography (DCM/EtOH = 50: 1, v/v) to obtain solid. The TEOS (2.0 mL) was dissolved in ethanol of 2.0 mL, then 20 mg of the above solids were added to the mixture one by one, then a few drops of triethanolamine were added drop by drop, and stirred for 1 hour. Thereafter, the product was collected by centrifugation and washed several times with ethanol to remove the residual reactants. The surface of silica nanoparticles was functionalized with carboxyl groups by co-condensation method. The reactant was completely dissolved in ethanol, and then glutaric anhydride was gradually added, stirred for 3 hours, centrifuged and washed away unreacted glutaric anhydride. The carboxyl functional two-photon fluorescent silica nanoparticles (TP-SiNPs) were obtained by freeze-drying.

Mouse liver was collected from a healthy mouse and cut into slices with the thickness of 400 μm . For imaging of TP-SiNPs in the slices, the slices were incubated with TP-SiNPs (400 $\mu\text{g}/\text{mL}$) for 4 h, washed with DPBS three times, and observed using Olympus FV1200MPE multiphoton laser scanning confocal microscope. The excitation wavelength of the femtosecond laser was set at 740 nm for imaging.

10. MRI response of the nanoprobe Tf-AuNCs@MnO₂ toward GSH in buffer solution and endogenous GSH in cells

The MRI response signals of the nanoprobe Tf-AuNCs@MnO₂ to different concentration of GSH were measured at 0.5 T on an MesoMR23-060H-I equipment. Glutathione at concentrations of 0, 0.5, 1.0, 1.5, 2.0 mM reacted with the nanoprobe Tf-AuNCs@MnO₂ for 10 min, and then the relaxation times and T₁-weighted signals images of the solution were measured on an MRI analysing and imaging system.

For the magnetic resonance imaging experiment of endogenous GSH, the cell processing method was the same as that of fluorescence imaging. The difference was that finally the cells incubated with the nanoprobe were centrifuged, the supernatant

was taken out, and then a 2.0 % agarose solution was added. The T₁-wighted signals images of the MCF-7 cells was measured on an MRI imaging machine.

11. Supplementary figures and table

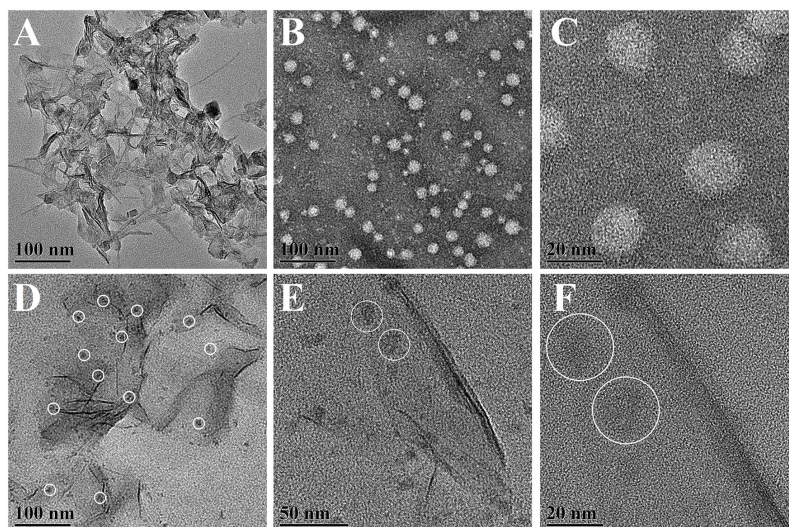


Fig. S1. TEM images of MnO₂ nanosheets (A) and Tf-AuNCs (B). HRTEM images of the Tf-AuNCs (C). TEM images of the nanoprobe Tf-AuNCs@MnO₂ (D), (E). HRTEM image of the nanoprobe Tf-AuNCs@MnO₂ (F).

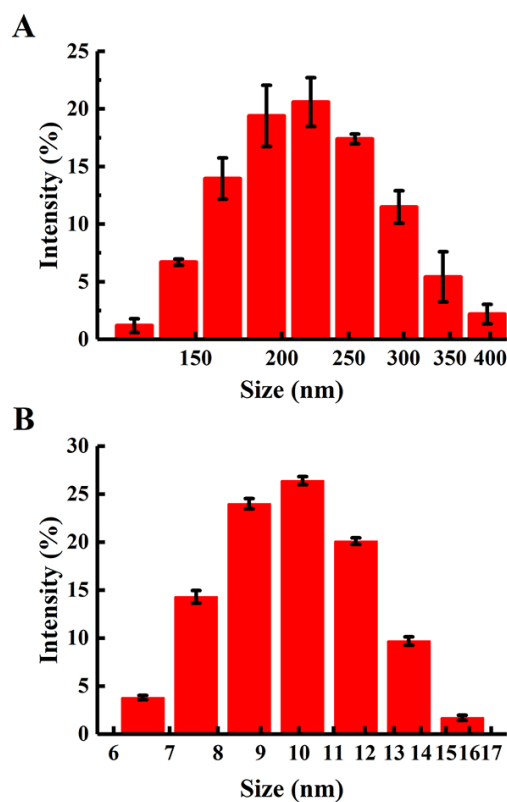


Fig. S2. (A) The histograms of particles size distribution of MnO₂ nanosheets by DLS. (B) The histograms of particles size distribution of Tf-AuNCs by DLS.

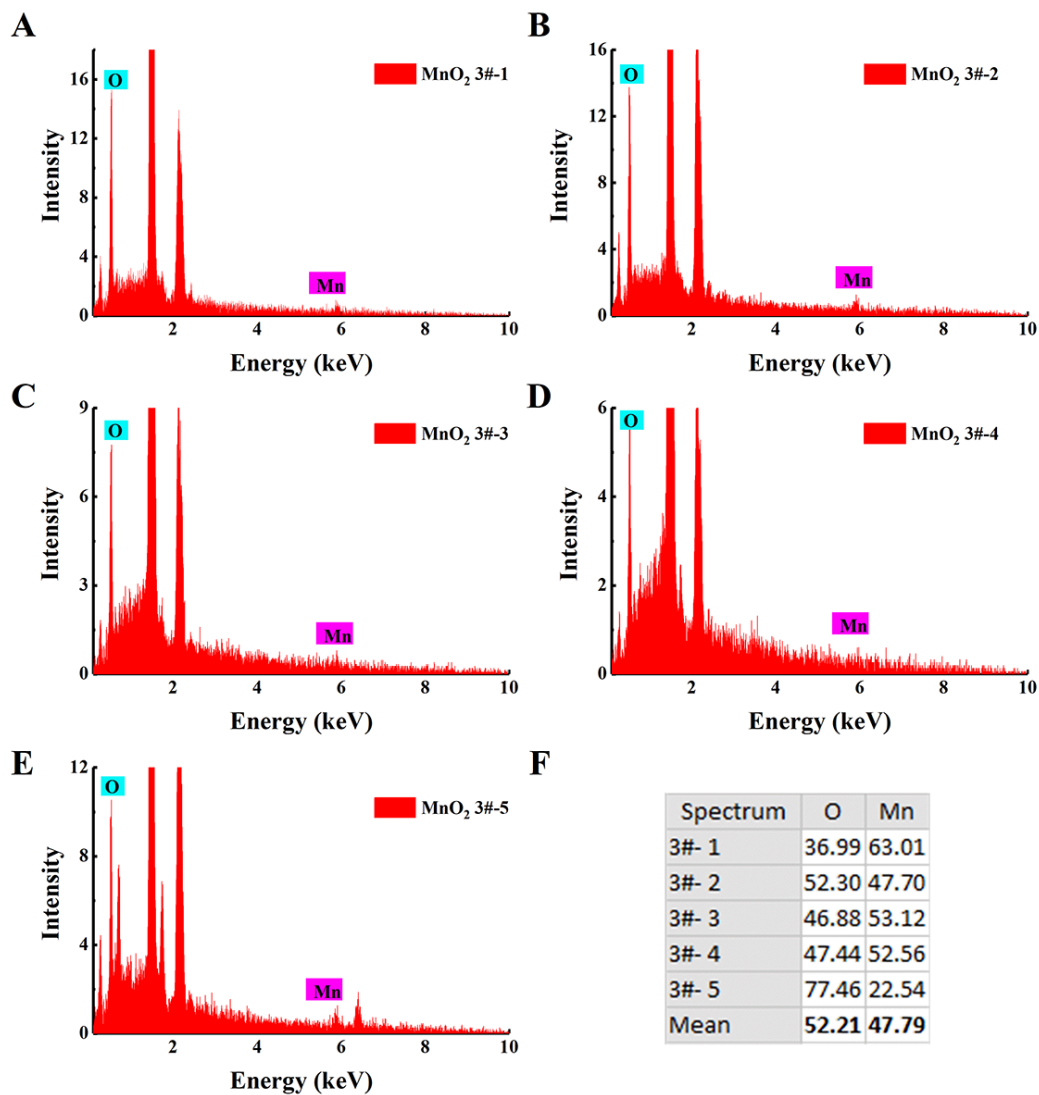


Fig. S3. (A), (B), (C), (D) and (E) are parallel EDS analysis of MnO_2 nanosheets. (F) The normalized mass percentage of each element of MnO_2 nanosheets.

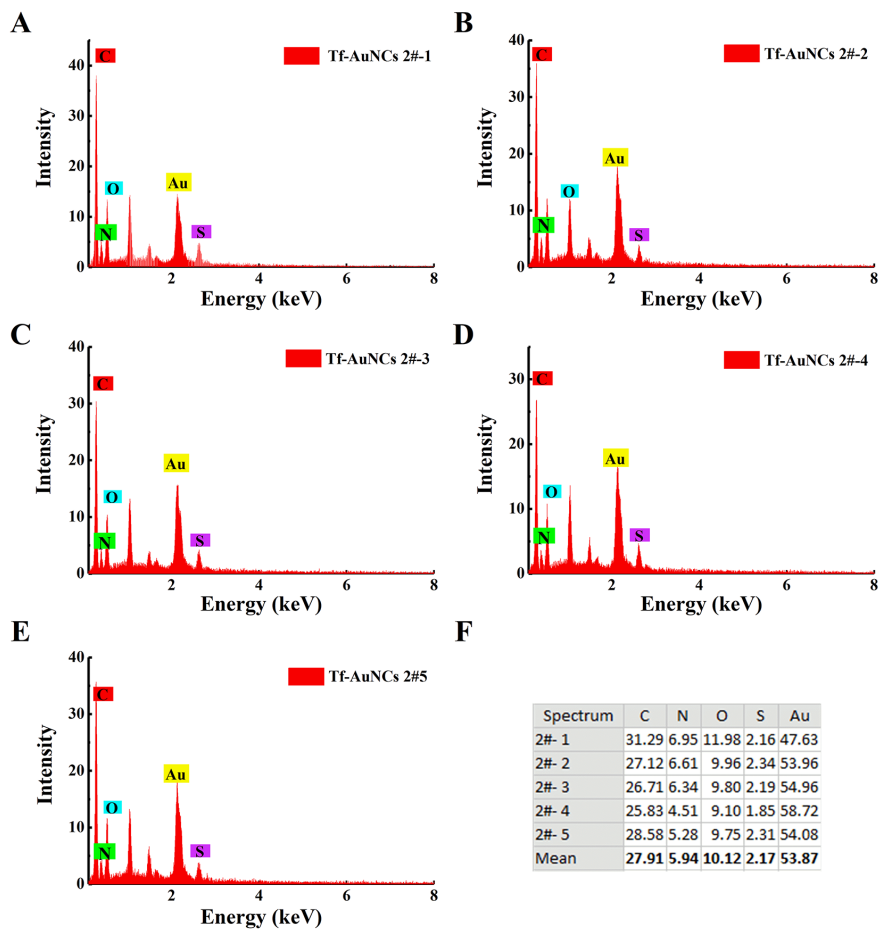


Fig. S4. (A), (B), (C), (D) and (E) are parallel EDS analysis of Tf-AuNCs. (F) The normalized mass percentage of each element of Tf-AuNCs.

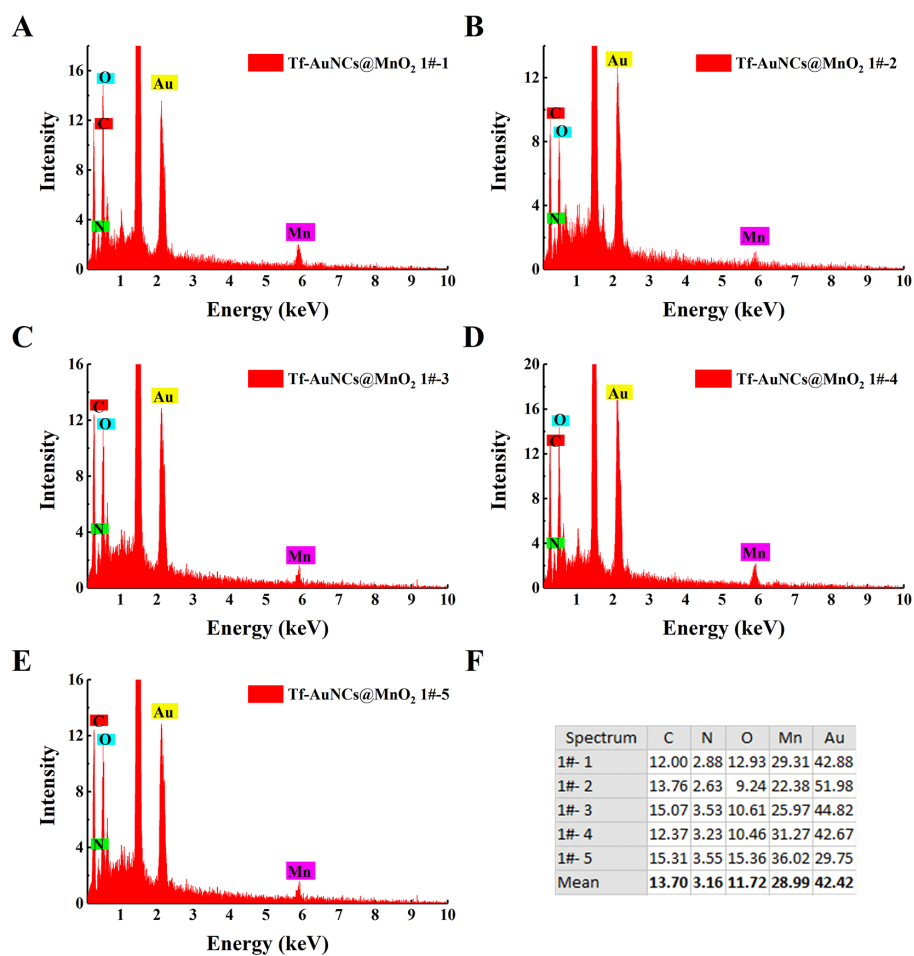


Fig. S5. (A), (B), (C), (D) and (E) are parallel EDS analysis of nanoprobe Tf-AuNCs@MnO₂. (F) The normalized mass percentage of each element of nanoprobe Tf-AuNCs@MnO₂.

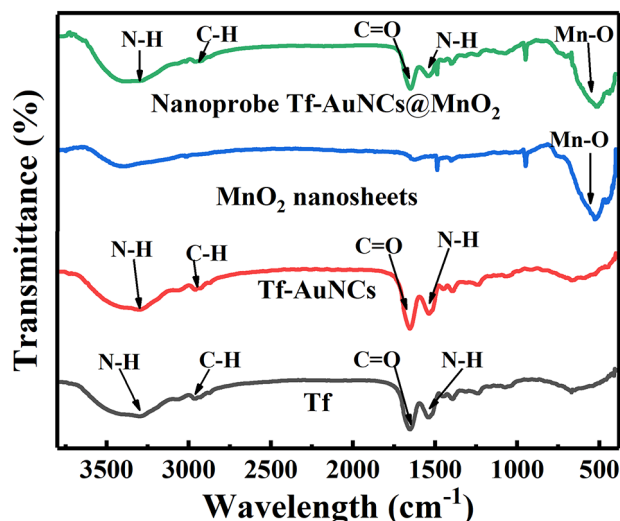


Fig. S6. FT-IR spectra of Tf (black line), Tf-AuNCs (red line), MnO₂ nanosheets (blue line), and nanoprobe Tf-AuNCs@MnO₂ (green line).

By comparing the FT-IR spectra of Tf and Tf-AuNCs, it is found that the functionalization of AuNCs by Tf causes the vibration peaks of the amide bond in Tf (C=O 1658 cm⁻¹, N-H 1544 cm⁻¹) to shift. Because the interaction of Tf and Au leads to changes in protein skeleton structure. In addition, the FT-IR spectrum of Tf-AuNCs showed a characteristic band of primary amine at 3306 cm⁻¹, and a broad band of C-H vibration at 2963 cm⁻¹. In the FT-IR spectrum of MnO₂, the characteristic stretching vibration peak of Mn-O at 515 cm⁻¹.

Table S1. Specific surface area of MnO₂ nanosheets with Brunauer-Emmett-Teller (BET) method.

Sample	Specific surface area (m ² /g)
MnO ₂ nanosheets	1.468

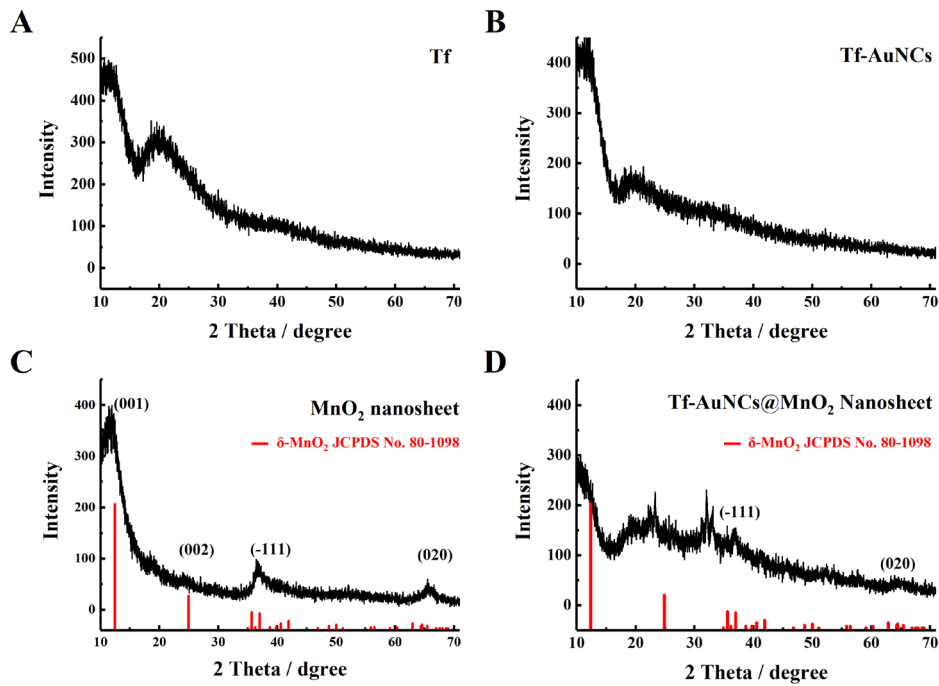


Fig. S7. XRD pattern of Tf (A), Tf-AuNCs (B), MnO₂ nanosheets (C) and nanoprobe Tf-AuNCs@MnO₂ (D).

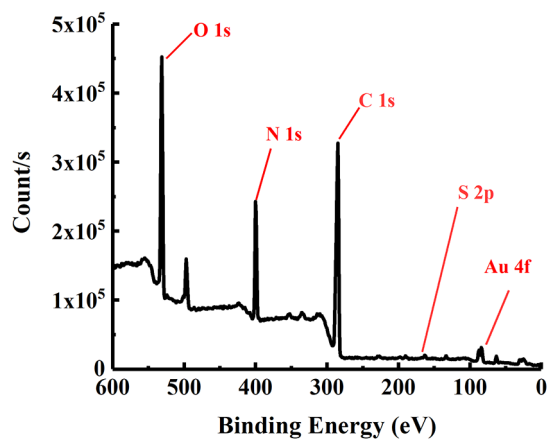


Fig. S8. XPS spectra of Tf-AuNCs (C 1s, O 1s, N 1s, S 2p, Au 4f).

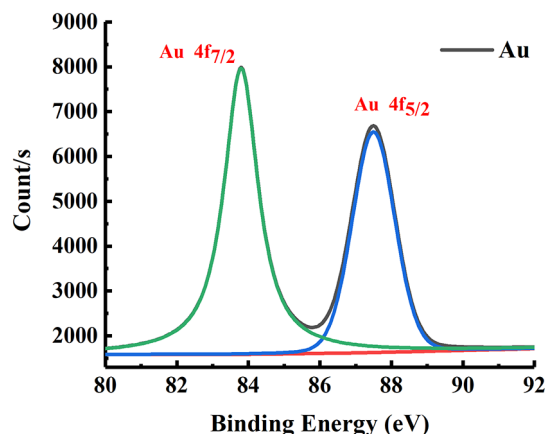


Fig. S9. High-resolution XPS of Au 4f for the Tf-AuNCs (Au 4f_{5/2}: 87.5 eV, Au 4f_{7/2}: 83.8 eV).

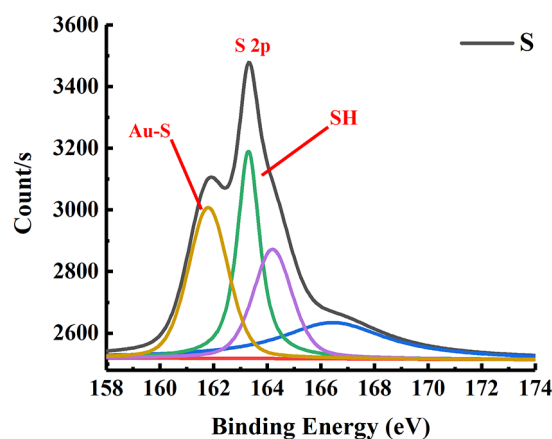


Fig. S10. High-resolution XPS of S 2p for the Tf-AuNCs (Au-S: 161.8 eV).

The properties of Tf-AuNCs were studied by X-ray photoelectron spectroscopy (XPS). As shown in Fig. S8, there are five types of XPS peaks in Tf-AuNCs: C 1s, O 1s, N 1s, S 2p, Au 4f. The Au 4f peak exhibited two distinct split energy levels (Fig. S9), indicating that during the reaction, the gold, whose valence state was trivalent, was completely changed to zero valence. The S 2p_{3/2} peak at 161.8 eV (Fig. S10) corresponding to a gold thiolate also confirmed the covalent interaction of AuNCs with the sulfhydryl group of transferrin.

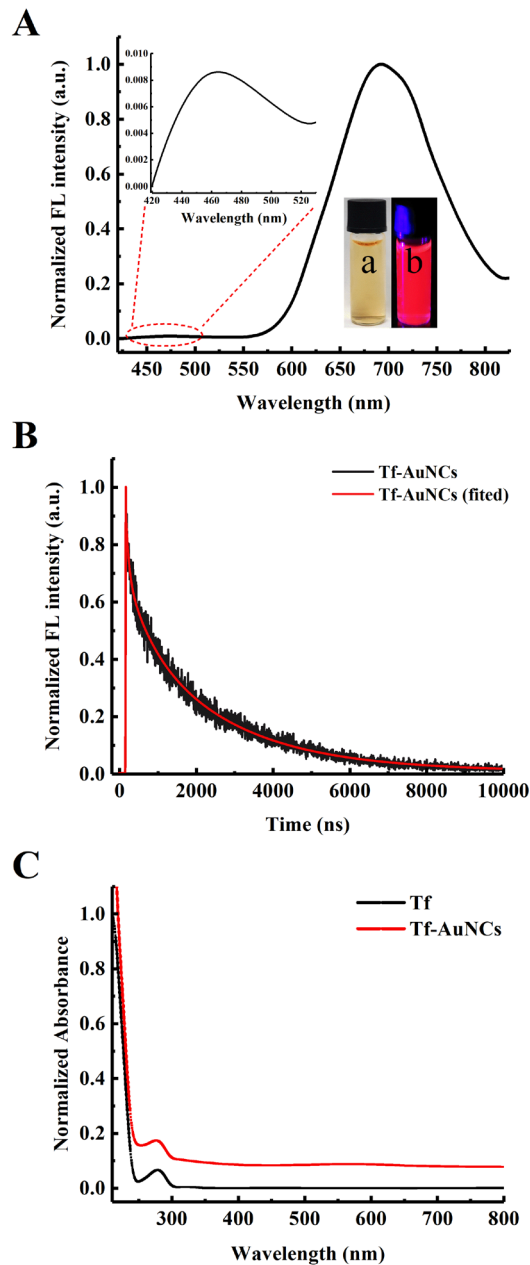


Fig. S11. (A) Normalized fluorescence emission spectra of the Tf-AuNCs ($\lambda_{\text{ex}}=360$ nm, $\lambda_{\text{em}}=681$ nm). Inset: the enlarged fluorescence spectra of Tf-AuNCs from 420 nm to 520 nm. Photographs of the Tf-AuNCs under (a) visible light and (b) the irradiation of ultraviolet light at 365 nm. (B) Fluorescence lifetime of Tf-AuNCs in PBS buffer solution (pH=7.4). (C) Normalized UV–Vis absorption spectra of Tf (black line) and Tf-AuNCs (red line).

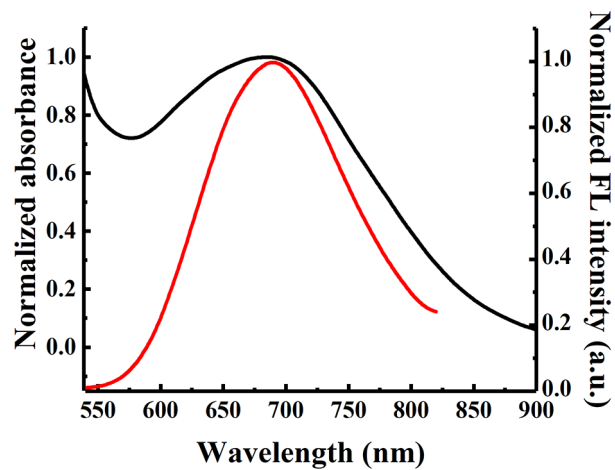


Fig. S12. Normalized UV-Vis absorption spectrum of MnO₂ nanosheets (black line) and normalized fluorescence emission spectra of the Tf-AuNCs (red line).

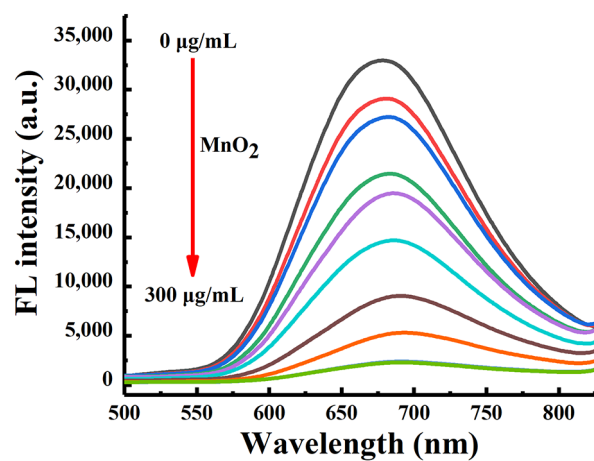


Fig. S13. Fluorescence emission spectra of the Tf-AuNCs (2.0 mg/mL) with different concentrations of MnO₂ nanosheets.

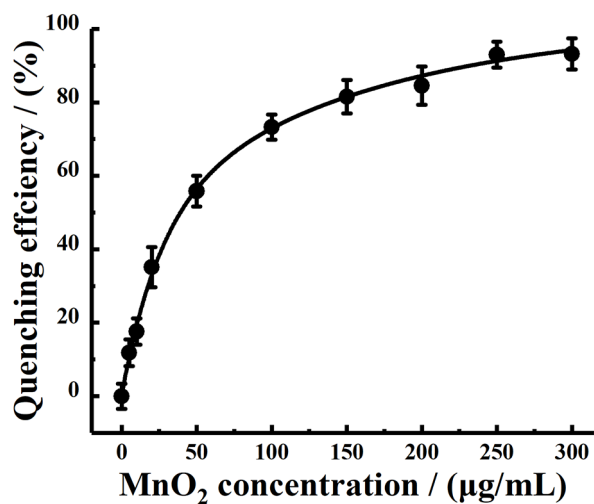


Fig. S14. Fluorescence quenching efficiency of MnO₂ nanosheets with Tf-AuNCs (2.0 mg/mL).

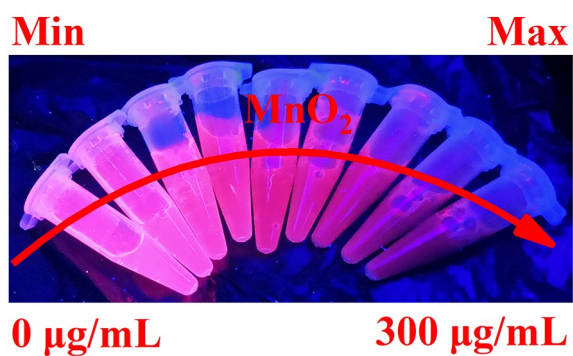


Fig. S15. Photographs of the Tf-AuNCs solutions with different concentrations of MnO₂ excited under 365 nm ultraviolet light.

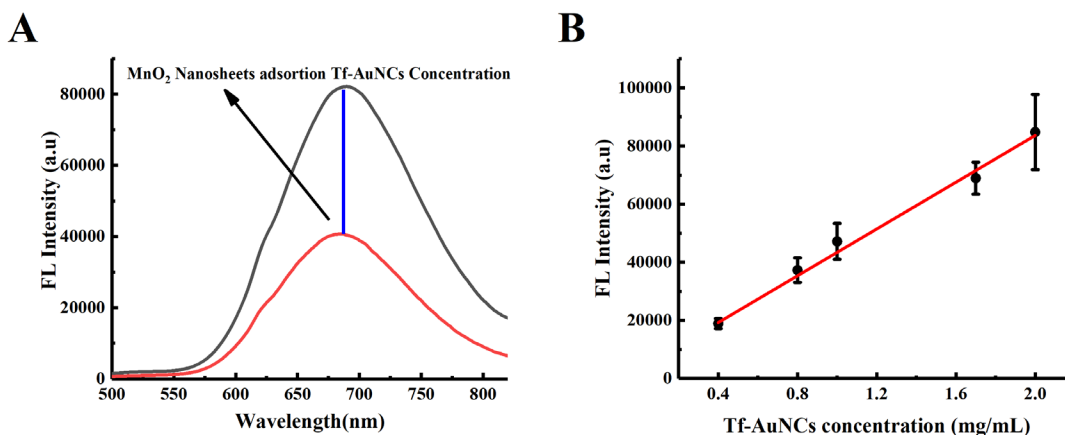


Fig. S16. (A) The changes of fluorescence intensity of Tf-AuNCs in the supernatant before (black line) and after (red line) Tf-AuNCs is absorbed by MnO₂ nanosheets (300 μg/mL). (B) Linear relationship between fluorescence intensity and different concentration of Tf-AuNCs.

The formula for calculating the adsorption of Tf-AuNCs by MnO₂ nanosheets is as follows:

$$I_Y = I_2 - I_1$$

$$I_Y = 82417.42482 - 40408.55725 = 42008.86757$$

I_Y : the fluorescence intensity of Tf-AuNCs absorbed on the MnO₂ nanosheets.

I_2 : before Tf-AuNCs were absorbed by MnO₂, the fluorescence intensity of Tf-AuNCs in the supernatant.

I_1 : after Tf-AuNCs were absorbed by MnO₂, the fluorescence intensity of Tf-AuNCs in the supernatant.

The equation of the standard curve of the fluorescence intensity of Tf-AuNCs at different concentrations is:

$$Y = 40224.43027X + 3184.77743 \quad (R^2 = 0.99003)$$

$$C_{\text{Tf-AuNCs}} = (I_Y - 3184.77743) / 40224.43027 = 0.96519 \text{ mg/mL}$$

$$M_{\text{ad}} = C_{\text{Tf-AuNCs}} : C_{\text{MnO}_2} = 0.96519 \text{ mg/mL} : 300 \text{ μg/mL} = 3.22 \text{ mg/mg} \cdot \text{MnO}_2$$

$C_{\text{Tf-AuNCs}}$: the concentration of Tf-AuNCs absorbed on the MnO₂ nanosheets.

C_{MnO_2} : the concentration of MnO₂ nanosheets.

M_{ad} : 1.0 mg of MnO₂ adsorbs the amount of Tf-AuNCs.

The calculation formula for the adsorption efficiency of MnO₂ nanosheets to adsorb Tf-AuNCs is as follows:

$$\eta = C_a / C_e$$

$$\eta = (0.96519 \text{ mg/mL}) / (2.0 \text{ mg/mL}) = 48.26\%$$

η : the adsorption efficiency of MnO₂ nanosheets.
 C_a : MnO₂ nanosheets absorption concentration of the Tf-AuNCs.
 C_e : Initial concentration of Tf-AuNCs.

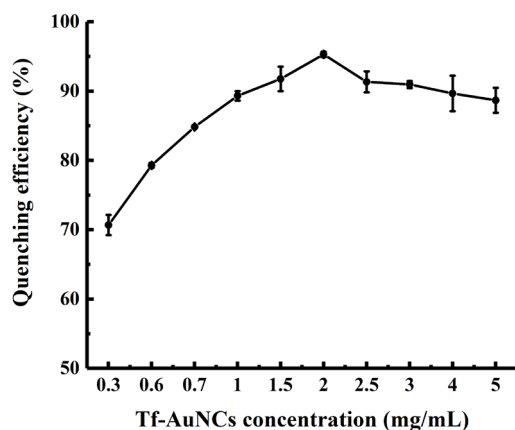


Fig. S17. The quenching efficiency of MnO₂ nanosheets to different concentrations of Tf-AuNCs.

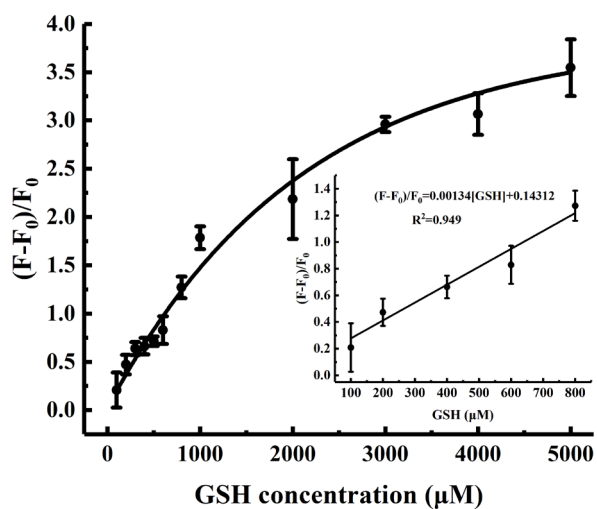


Fig. S18. Relationship between fluorescence enhancement and GSH concentration. F_0 and F are the fluorescence intensity of nanoprobe Tf-AuNCs@MnO₂ (Tf-AuNCs concentration was 0.6 mg/mL) in the absence and presence of GSH, respectively. (Insert figure: Linear relationship between fluorescence intensity recovery ratio and GSH concentration).

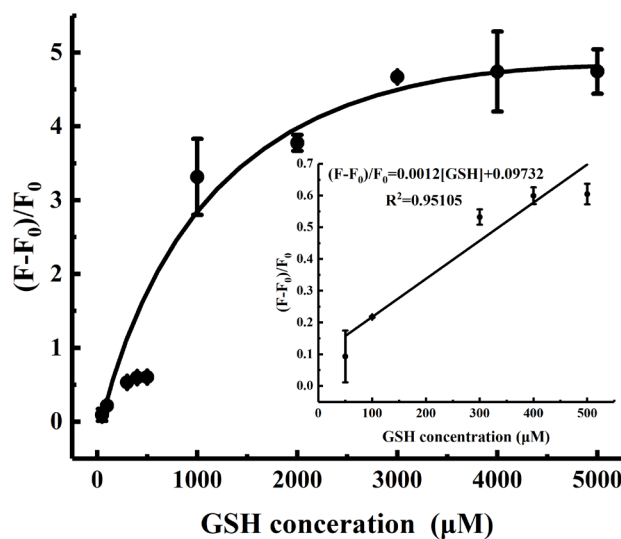


Fig. S19. Relationship between fluorescence enhancement and GSH concentration. F_0 and F are the fluorescence intensity of nanoprobe Tf-AuNCs@MnO₂ (Tf-AuNCs concentration was 1.0 mg/mL) in the absence and presence of GSH, respectively. (Insert figure: Linear relationship between fluorescence intensity recovery ratio and GSH concentration).

To explain whether the detection limit and response range of change with the concentration change of Tf-AuNCs, the concentration of Tf-AuNCs in nanoprobe was selected as 0.6 mg/mL (Fig. S18) and 1.0 mg/mL (Fig. S19) to respond GSH. The detection limits of the two nanoprobe were 169 μM (0.6 mg/mL), 366 μM (1.0 mg/mL) respectively. Due to the fluorescence quenching efficiency of these two nanoprobe (0.6, 1.0 mg/mL) was reduced, the lower detection limit of GSH became worse than the detection limit of Tf-AuNCs@MnO₂ (2.0 mg/mL, 16 μM). The range of response (0-5.0 mM) has not changed much.

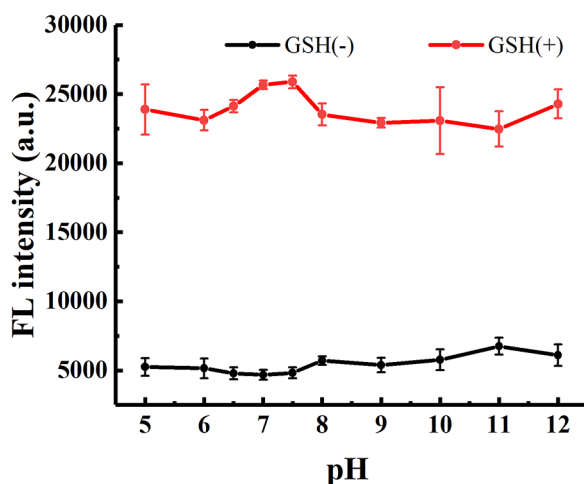


Fig. S20. (A) Effect of pH on the fluorescence intensity of the nanoprobe Tf-AuNCs@MnO₂ (300 μg/mL). (Red line: presence GSH. Black line: absence GSH). Fluorescence intensity was recorded at 681 nm with an excitation wavelength of 460 nm.

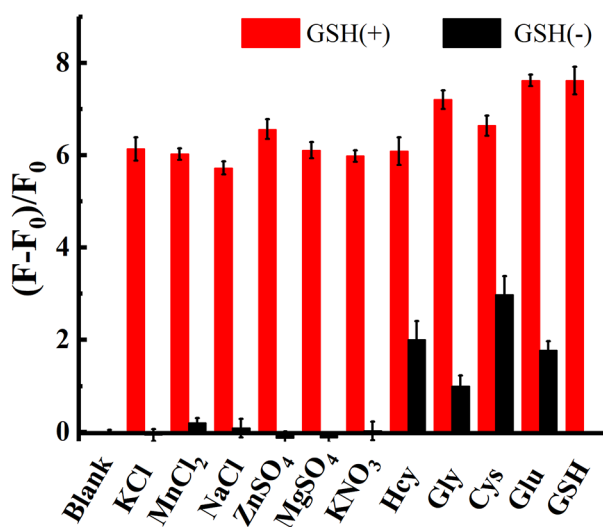


Fig. S21. Fluorescence responses of the nanoprobe Tf-AuNCs@MnO₂ to different interfering agents (MnCl₂, NaCl, ZnSO₄, MgSO₄, KNO₃, Hcy, Gly, Cys, Glu, respectively, concentration:0.5 mM).

To evaluate specificity of the Tf-AuNCs@MnO₂ to GSH in buffer solution, the effect of various interfering species (KCl, MnCl₂, NaCl, ZnSO₄, MgSO₄, KNO₃, Hcy, Gly, Cys, Glu), which coexisted with GSH, were explored. The FL intensity of the

nanoprobe was only remarkably enhanced for the presence of GSH. It worth nothing that three amino acids of Hcy, Cys, and Glu caused fluorescence of Tf-AuNCs@MnO₂ nanoprobe to recover to a certain extent. The concentration of GSH was considerably higher than that of three amino acids (Hcy, Cys, and Glu) in mammalian cells, so it would not affect the detection of intracellular GSH.^{1,2}

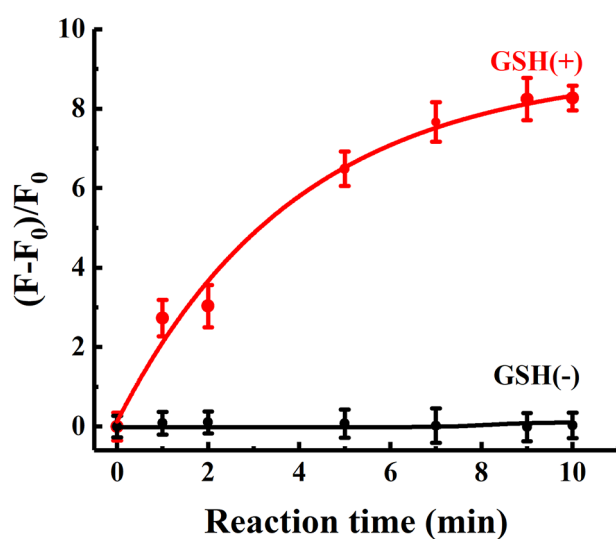


Fig. S22. Effect of reaction time on the fluorescence intensity of nanoprobe Tf-AuNCs@MnO₂ (300 μ g/mL) to GSH (4.0 mM). Reactions were performed at 25°C in PBS (pH=7.4). Red line: presence GSH. Black line: absence GSH.

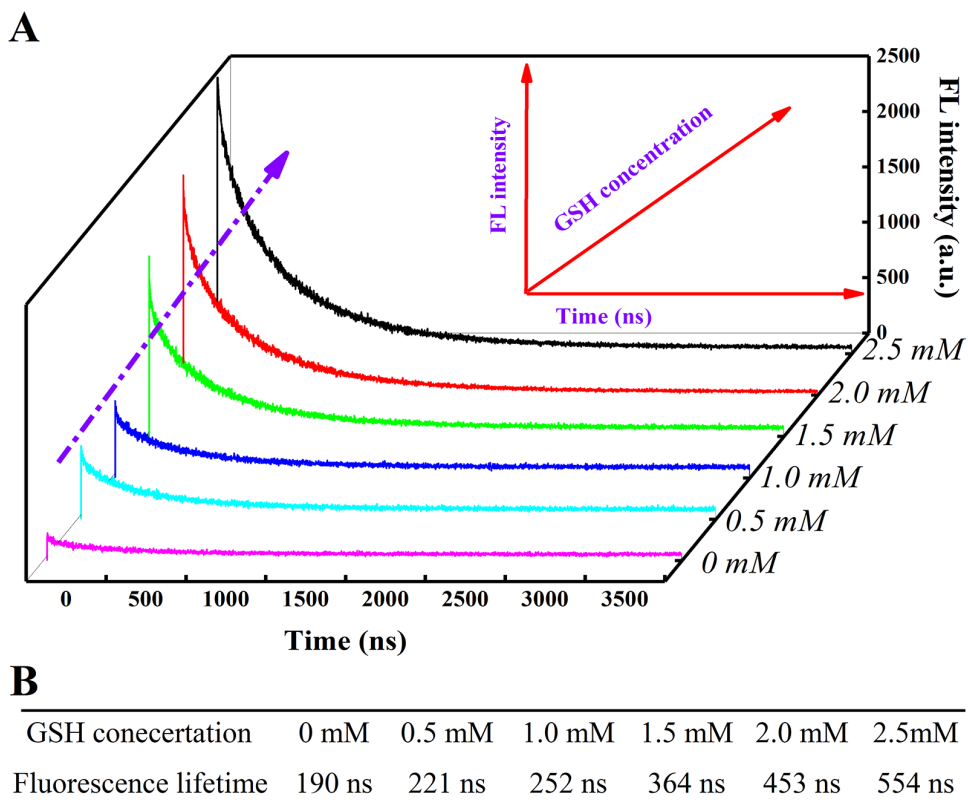


Fig. S23. (A) Fluorescence lifetime decay curves of the nanoprobe Tf-AuNCs@MnO₂ (300 μg/mL) in the presence of different concentrations of GSH. (B) The fluorescence lifetime value of nanoprobe Tf-AuNCs@MnO₂ with different GSH concentration.

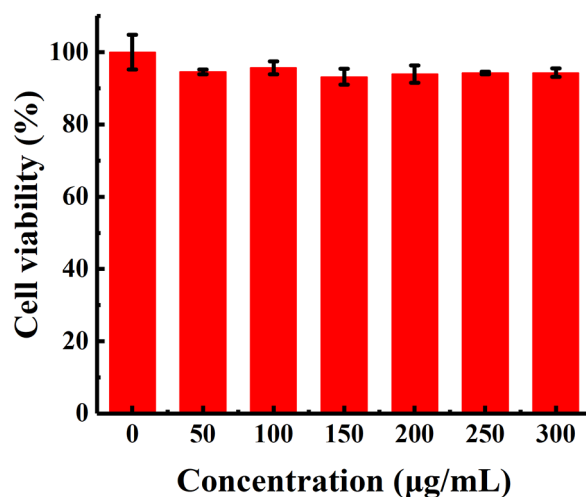


Fig. S24. Cell viability of MCF-7 cells after being incubated with different concentrations of the nanoprobe Tf-AuNCs@MnO₂ for 24 h.

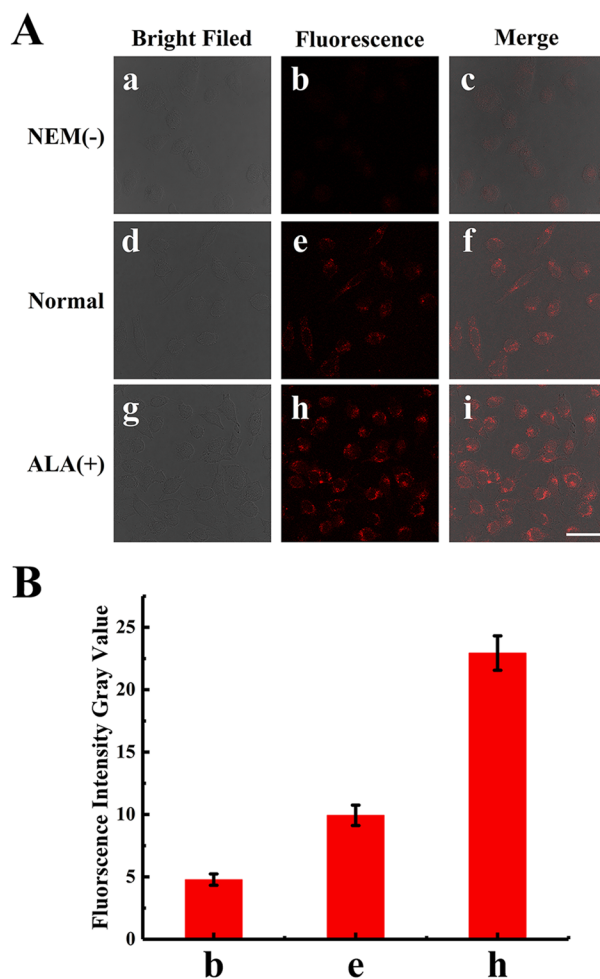


Fig. S25. (A) Single-photon confocal fluorescence imaging of endogenous GSH in MCF-7 cells treated with the nanoprobe Tf-AuNCs@MnO₂ (300 μg/mL). (a-c) NEM pre-treated MCF-7 cells incubated with Tf-AuNCs@MnO₂ nanoprobe. (d-f) Untreated MCF-7 cells incubated with Tf-AuNCs@MnO₂ nanoprobe (control). (g-i) ALA pre-treated MCF-7 cells incubated with Tf-AuNCs@MnO₂ nanoprobe. (B) Fluorescence intensity gray value of single-photon confocal fluorescence imaging in MCF-7 cells. Fluorescence intensity gray value of NEM (b) and ALA (h) pre-treated MCF-7 cell images. Fluorescence intensity grey value of untreated (e) MCF-7 cell images. Scale bar=50 μm. λ_{ex}=488 nm. λ_{em}=620-780 nm.

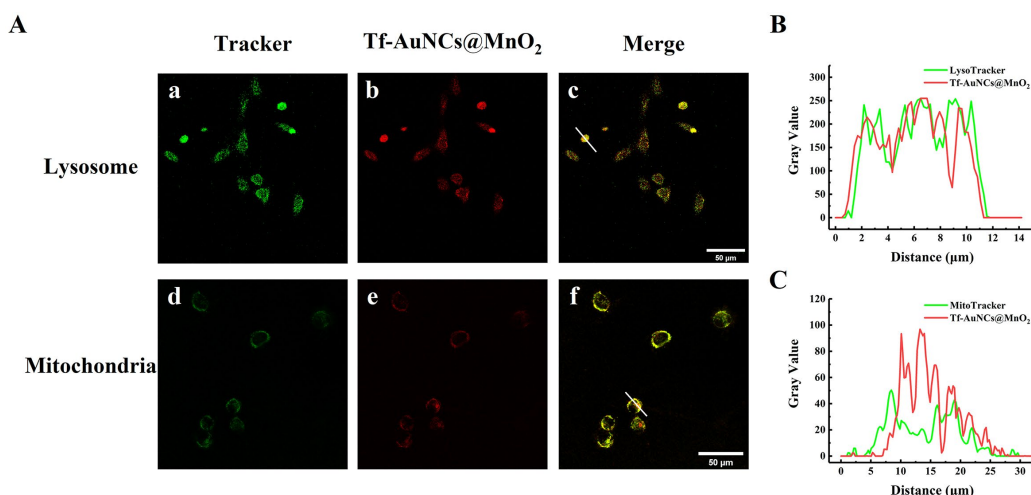


Fig. S26. (A) Subcellular colocalization images of Tf-AuNCs@MnO₂ in MCF-7 cells with lysoTracker ($\lambda_{\text{ex}}=488$ nm, $\lambda_{\text{em}}=500\text{-}540$ nm) and MitoTracker ($\lambda_{\text{ex}}=488$ nm, $\lambda_{\text{em}}=500\text{-}540$ nm). Tf-AuNCs@MnO₂ ($\lambda_{\text{ex}}=488$ nm, $\lambda_{\text{em}}=620\text{-}780$ nm), Scale bar=50 μm . (B) Intensity profiles for region of interest (white line in the image (c)) on Tf-AuNCs@MnO₂ (red) and lysoTracker (green) distributed in MCF-7 cells. (C) Intensity profiles for region of interest (white line in the image (f)) on Tf-AuNCs@MnO₂ (red) and MitoTracker (green) distributed in MCF-7 cells.

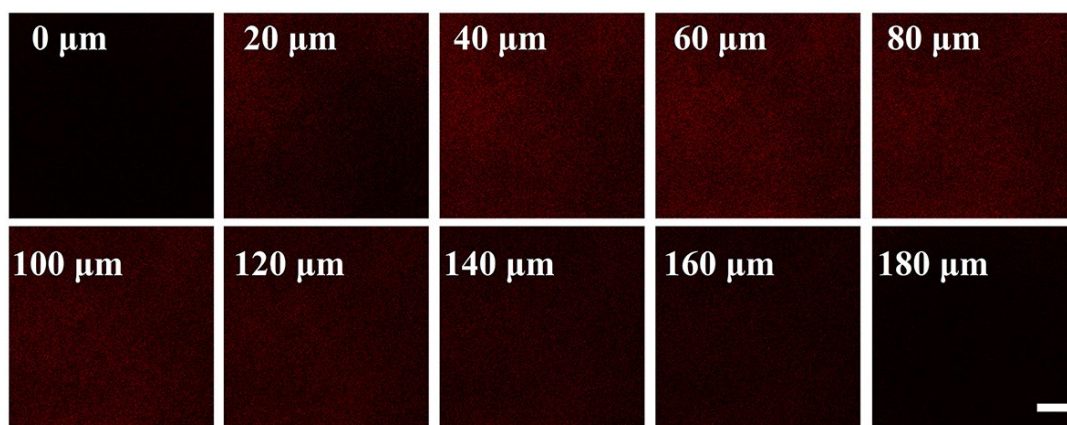


Fig. S27. Depth single-photon fluorescence images of the nanoprobe Tf-AuNCs@MnO₂ (300 $\mu\text{g}/\text{mL}$) in mouse liver tissue. The change of fluorescence intensity with scan depth were determined by single-photon confocal fluorescence in the Z-scan mode (step size, 20 μm). Scale bar=200 μm . $\lambda_{\text{ex}}=488$ nm, $\lambda_{\text{em}}=620\text{-}780$ nm.

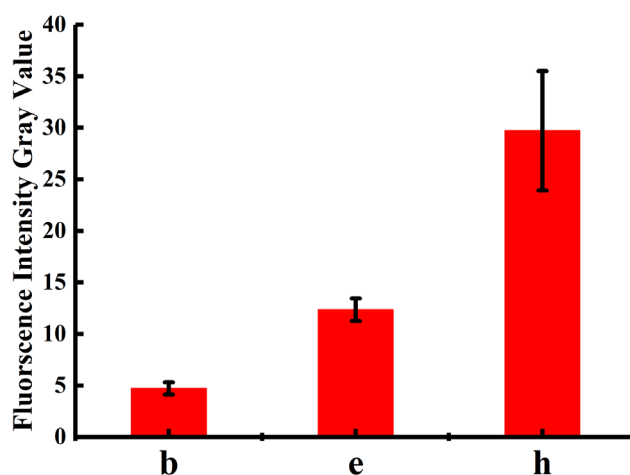


Fig. S28. Fluorescence intensity gray value of two-photon fluorescence imaging in MCF-7 cells. Fluorescence intensity grey value of NEM (b) and ALA (h) pretreated MCF-7 cell images. Fluorescence intensity gray value of untreated (e) MCF-7 cell images.

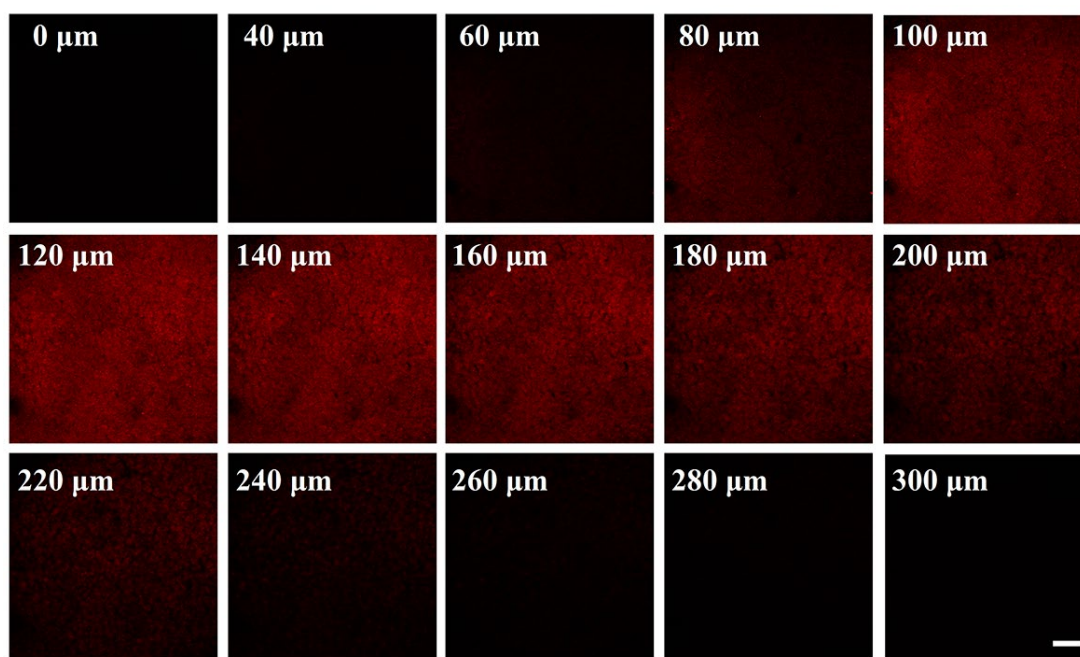


Fig. S29. Depth two-photon fluorescence images of nanoprobe Tf-AuNCs@MnO₂ (3.0 mg/mL) in mouse liver tissue. The change of fluorescence intensity with scan depth were determined by two-photon confocal fluorescence microscopy in the Z-scan mode (step size, 20 μm). Scale bar=200 μm. λ_{ex} =920 nm. λ_{em} =620-780 nm.

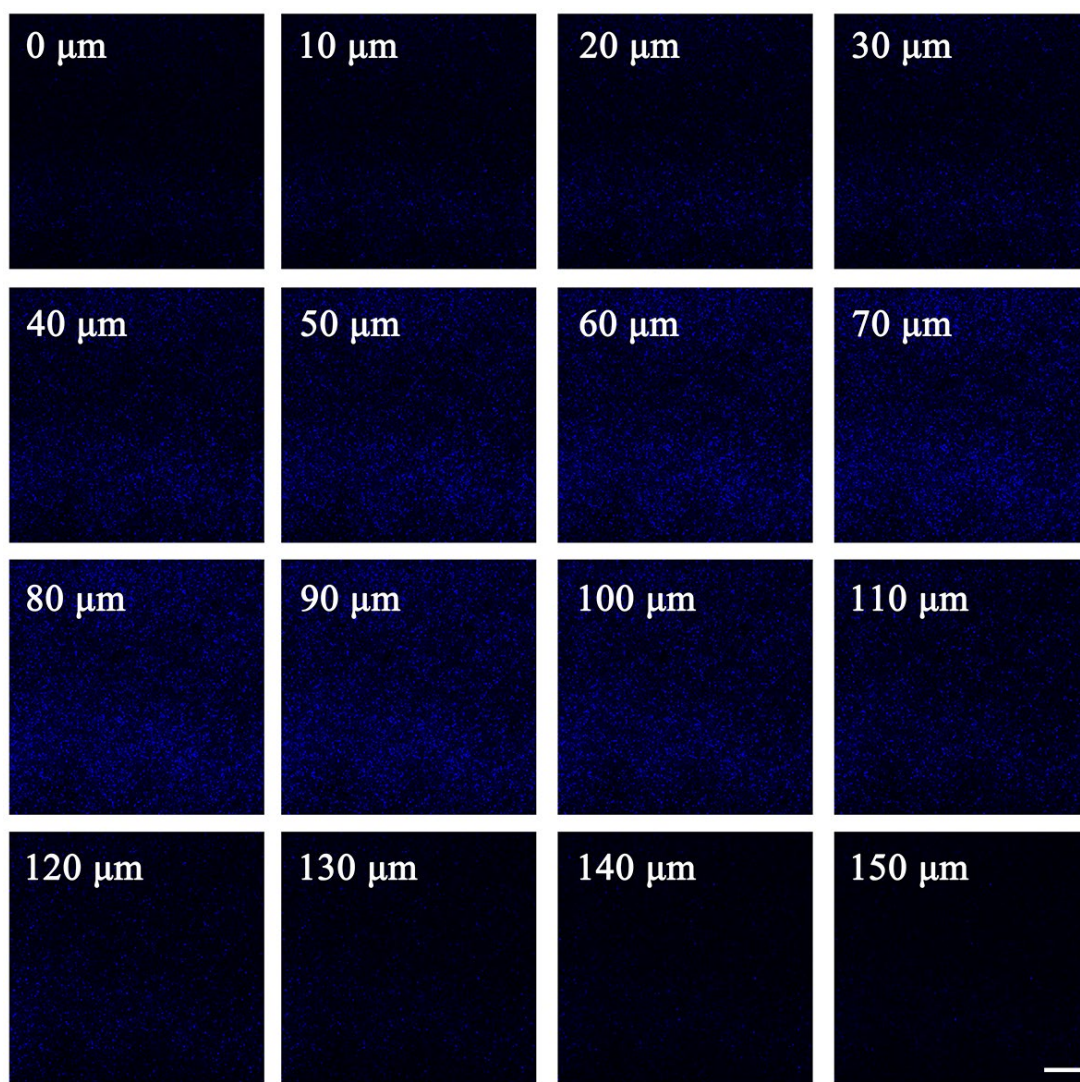


Fig. S30. Depth two-photon fluorescence images of TP-SiNPs (500 µg/mL) in mouse liver tissue. The change of fluorescence intensity with scan depth were determined by two-photon confocal fluorescence microscopy the Z-scan mode (step size, 10 µm). Scale bar=50 µm. $\lambda_{\text{ex}}=740$ nm, $\lambda_{\text{em}}=420-480$ nm.

12. References

1. W. Shi, B. Song, W. Shi, X. Qin, Z. Liu, M. Tan, L. Wang, F. Song and J. Yuan, *ACS Appl. Mater. Interfaces*, 2018, **10**, 27681-27691.
2. S. Zhu, S. Wang, M. Xia, B. Wang, Y. Huang, D. Zhang, X. Zhang and G. Wang, *ACS Appl. Mater. Interfaces*, 2019, **11**, 31693-31699.